

Proximity effect of a ferromagnetic insulator in contact with a superconductor

T. Tokuyasu*

Joseph Henry Laboratories of Physics, Jadwin Hall, Princeton University, Princeton, New Jersey 08544

J. A. Sauls

Department of Physics and Astronomy, Northwestern University, Evanston, Illinois 60208

D. Rainer

Physikalisches Institut der Universität Bayreuth, D-8580 Bayreuth, Federal Republic of Germany

(Received 23 March 1988)

We propose a model for conventional superconductors in contact with a ferromagnetic (or polarized paramagnetic) insulator. The model is defined by a boundary condition on the quasiclassical Green's function for the superconductor at the interface between the metal and insulating magnet. The specific boundary condition we use describes the interaction of the electrons, which tunnel into the insulating barrier, with the average exchange field of the local moments. Solutions to the quasiclassical equations and boundary condition are obtained for thin superconducting films. We obtain results for pair-breaking effects of a magnetic boundary on the transition temperature and gap of thin superconducting films. Of particular interest is the Zeeman effect in the quasiparticle density of states (DOS), which exhibits a splitting of the form $2\mu_c(H + B^*)$ in an external field H . The excess splitting B^* is interpreted here as an internal field in the superconductor resulting from quasiparticle tunneling into the magnetic insulator, and subsequent reflection into the superconducting film. We compare our model of the tunneling DOS with the recent measurements by Tedrow *et al.* on EuO/Al/Al₂O₃ tunnel junctions.

I. INTRODUCTION

Advances in the fabrication of thin films and artificial superlattices have led to new investigations into the interaction of superconductivity and magnetism. Wong *et al.*¹ have measured the parallel upper critical field of magnetic superconducting sandwiches and superlattices made of V and Fe, and interpret their data in terms of a crossover from two-dimensional (2D) to three-dimensional (3D) superconductivity, suggesting the coexistence of V superconductivity and Fe ferromagnetism. SIS junctions made of Pb and Ho(OH)₃ (which is ferromagnetic in bulk form) show a threefold splitting in the conductance versus voltage.² Stageberg *et al.*² proposed that this splitting could be explained by a surface bound state of the pair potential, which is depressed by the magnetic Ho(OH)₃ barrier, and a Zeeman splitting of the conventional BCS conductance peak. DeWeert and Arnold² suggest that this bound state results from the exchange coupling of quasiparticles to the ions in the insulating ferromagnetic layer, although they do not rule out a bound state resulting from a spatial variation of the pair potential. Recently, Tedrow *et al.*³ carried out high-field tunneling measurements of the density of states (DOS) in superconducting films of Al backed by EuO, which in bulk form is a ferromagnetic insulator with a Curie temperature of 70 K and an optical gap of 1.1 eV.⁴ They observed a twofold spin-splitting of the DOS in excess of the Zeeman energy $2\mu_c B$, which they interpret as an internal field of EuO acting on the Al conduction electrons. This is a remarkable effect given the semiclassical

picture of conduction electrons in pure Al traveling along classical trajectories and being reflected specularly by a smooth interface with an insulator,

The quasiclassical (QC) theory of superconductivity,⁵ formulated by Eilenberger, Larkin, and Ovchinnikov, and Eliashberg, is powerful enough to deal with superconductivity in restricted geometries such as proximity contacts. However, in order to deal with the complications imposed by interfaces between superconductors and other materials, interface boundary conditions must be added to the original formulation of the QC theory. The correct boundary condition depends on the details of the interface, e.g., roughness, reflectivity, magnetic properties, etc. The boundary conditions that have so far been proposed for the QC equations are reviewed in Ref. 6.

In this paper we describe a theoretical model for a thin superconductor in contact with a polarized material, which may either be a ferromagnet or a paramagnet in an external field (see Fig. 1), and calculate some observable consequences of the theory. The model for the interface is described by a boundary condition on the QC Green's function, the propagator of the theory, and is formulated in Sec. III in terms of an interface scattering matrix, as described by Millis *et al.*⁷ In Sec. IV, we examine the effects of the boundary condition on the gap and exchange field induced in a superconductor near an insulating magnetic surface. We specialize the discussion to a thin superconducting film in contact with a magnetic surface (Sec. V), and in Secs. VI and VII calculate the surface-magnetic pairbreaking effect on the transition temperature as well as the tunneling density of states of

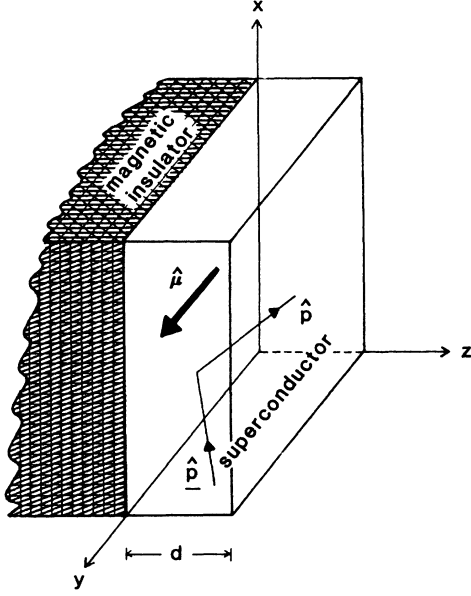


FIG. 1. Thin film geometry. A superconducting film of thickness $d \ll \xi_0$ is bounded by a magnetic insulator on the left and a nonmagnetic insulator on the right. The internal field of the magnetic material is taken to be along the y axis, and $\hat{\mathbf{p}}$ and $\hat{\mathbf{p}}'$ refer to trajectories for incoming and specular reflected quasiparticles.

the film. In Sec. VIII we compare the results for the thin film with the tunneling measurements of Tedrow *et al.*³ Readers less interested in the details of the calculations can skip to Sec. VI. We begin by briefly reviewing the relevant equations of the QC theory; for a more complete discussion see the articles by Alexander *et al.*⁵ and Serene and Rainer.⁸

II. QUASICLASSICAL EQUATIONS

The basic equations of the equilibrium QC theory are (1) the transport equation,

$$[i\epsilon_n \hat{\tau}_3 - \hat{\sigma} - \hat{\Delta}, \hat{\mathbf{g}}(\hat{\mathbf{p}}, \mathbf{R}; \epsilon_n)]_- + i\mathbf{v}_F \cdot \nabla_{\mathbf{R}} \hat{\mathbf{g}}(\hat{\mathbf{p}}, \mathbf{R}; \epsilon_n) = 0, \quad (1)$$

where $[\hat{\mathbf{A}}, \hat{\mathbf{B}}]_{\pm} = \hat{\mathbf{A}} \hat{\mathbf{B}} \pm \hat{\mathbf{B}} \hat{\mathbf{A}}$, (2) the normalization condition,

$$[\hat{\mathbf{g}}(\hat{\mathbf{p}}, \mathbf{R}; \epsilon_n)]^2 = -\pi^2 \hat{1}, \quad (2)$$

and (3) the self-energy equations that determine the (diagonal) self-energy, $\hat{\sigma}$, and the gap matrix, $\hat{\Delta}$ in terms of the QC propagator, $\hat{\mathbf{g}}$, and the relevant interactions of the theory. The propagator $\hat{\mathbf{g}}$ is a 4×4 Nambu matrix, representing both spin and particle-hole degrees of freedom, that depends upon $\hat{\mathbf{p}}$, the direction of the momentum of a quasiparticle on the Fermi surface, \mathbf{R} , the position variable, and the Matsubara frequencies, $\epsilon_n = (2n+1)\pi T$. Although it is not a limitation of the QC theory, we assume a spherical Fermi surface, in which case the Fermi velocity \mathbf{v}_F is directed along $\hat{\mathbf{p}}$.

The physical solutions of Eqs. (1) and (2) must satisfy

the self-consistency equations determining $\hat{\Delta}(\hat{\mathbf{p}}, \mathbf{R}; \epsilon_n)$ and the diagonal self-energy $\hat{\sigma}(\hat{\mathbf{p}}, \mathbf{R}; \epsilon_n)$. In the weak-coupling theory the self-consistency equation for $\hat{\Delta}$ is the BCS mean-field gap equation,

$$\hat{\Delta}(\hat{\mathbf{p}}, \mathbf{R}) = \int \frac{d\Omega}{4\pi} v(\hat{\mathbf{p}} \cdot \hat{\mathbf{p}}') T \sum_n \hat{\mathbf{f}}(\hat{\mathbf{p}}', \mathbf{R}; \epsilon_n), \quad (3)$$

where $v(\hat{\mathbf{p}} \cdot \hat{\mathbf{p}}')$ is the pairing interaction and $\hat{\mathbf{f}}(\hat{\mathbf{p}}, \mathbf{R}; \epsilon_n)$ is the off-diagonal part of the propagator in particle-hole space,

$$\hat{\mathbf{g}}(\hat{\mathbf{p}}, \mathbf{R}; \epsilon_n) = \begin{bmatrix} g(\hat{\mathbf{p}}, \mathbf{R}; \epsilon_n) & f(\hat{\mathbf{p}}, \mathbf{R}; \epsilon_n) \\ f(-\hat{\mathbf{p}}, \mathbf{R}; \epsilon_n)^* & g(-\hat{\mathbf{p}}, \mathbf{R}; -\epsilon_n)^{\text{tr}} \end{bmatrix}, \quad (4)$$

with spin dependence of the diagonal (g) and off-diagonal (f) amplitudes given by

$$g = g_s + \mathbf{g} \cdot \boldsymbol{\sigma}, \quad f = f_0 i \sigma_2 + \mathbf{f} \cdot i \boldsymbol{\sigma} \sigma_2. \quad (5)$$

For conventional s -wave pairing, $v(\hat{\mathbf{p}} \cdot \hat{\mathbf{p}}') = v_0$ is constant and $\hat{\Delta}(\mathbf{R})$ depends only on the center-of-mass coordinate \mathbf{R} of the pairs. Also the gap matrix is of the form, $i\Delta \sigma_2 \tau_1$, where, by convenient choice of gauge, Δ may be chosen to be real, and σ_i and τ_j are Pauli matrices in spin space and particle-hole space, respectively. Strong-coupling corrections to the weak-coupling gap equation are small, down by factors of $T_c / \Omega_{\text{Debye}}$ and T_c / E_F , and neglected here; they may be included if necessary. The diagonal self-energy accounts for two other important effects in metals: (1) many-body effects described by Fermi-liquid molecular fields and (2) finite mean-free-path effects resulting from scattering of quasiparticles with impurities, phonons, or other quasiparticles. At low temperatures, $T \ll E_F$, Ω_{Debye} , impurity scattering typically dominates. However, for our applications we consider the clean limit in which the mean free path, $l = v_F \tau$, is large compared with coherence length ξ_0 . In this case the impurity self-energy may be neglected, so that

$$\hat{\sigma}(\hat{\mathbf{p}}, \mathbf{R}; \epsilon_n) = \hat{\sigma}_{\text{mf}}(\hat{\mathbf{p}}, \mathbf{R}) = \begin{bmatrix} \sigma(\hat{\mathbf{p}}, \mathbf{R}) & 0 \\ 0 & \sigma(-\hat{\mathbf{p}}, \mathbf{R})^{\text{tr}} \end{bmatrix}, \quad (6)$$

$$\sigma(\hat{\mathbf{p}}, \mathbf{R}) = T \sum_n \int \frac{d\Omega'}{4\pi} [A^s(\hat{\mathbf{p}} \cdot \hat{\mathbf{p}}') g_s(\hat{\mathbf{p}}', \mathbf{R}; \epsilon_n) + A^a(\hat{\mathbf{p}} \cdot \hat{\mathbf{p}}') \mathbf{g}(\hat{\mathbf{p}}', \mathbf{R}; \epsilon_n) \cdot \boldsymbol{\sigma}]. \quad (7)$$

For high-field tunneling, which we discuss in Sec. VIII, the most important Fermi-liquid correction is the electronic exchange interaction given by the isotropic part (A_0^g) of the interaction $A^a(\hat{\mathbf{p}} \cdot \hat{\mathbf{p}}')$. The resulting exchange field in the superconductor is

$$\mathbf{h} = A_0^g T \sum_n \int \frac{d\Omega}{4\pi} \mathbf{g}(\hat{\mathbf{p}}, \mathbf{R}; \epsilon_n), \quad (8)$$

which also contributes to the magnetization,

$$\mathbf{M} = 2N(E_F) \mu_e (1 - A_0^g) \left[\mu_e \mathbf{H} + T \sum_n \int \frac{d\Omega}{4\pi} \mathbf{g}(\hat{\mathbf{p}}, \mathbf{R}; \epsilon_n) \right], \quad (9)$$

where μ_e is the Bohr magneton, \mathbf{H} is an external field,

and $N(E_F)$ is the normal metallic density of states at the Fermi energy.

III. SMOOTH, PERFECTLY REFLECTING MAGNETIC BOUNDARIES

The QC equations for the propagator must be supplemented by boundary conditions (BC's) to describe the effects of finite geometries. Boundary conditions for smooth, magnetically active interfaces were recently discussed by Millis *et al.*⁷ These authors model the boundary as a high-energy potential barrier. Such potentials are outside the region of validity of the QC theory, and hence the specific form of the BC's must be developed from a microscopic theory. However, many general properties of the BC depend only on the symmetry properties of the interface potential. For a *smooth*, perfectly reflecting boundary, the scattering states of quasiparticles impinging on, and reflected from, such a boundary may be represented in terms of an interface, or boundary, S matrix which connects the incident "scattering in" quasiparticle state and reflected "scattering out" quasiparticle state. In particular, if $G(F)$ is the two-component spinor amplitude for the incoming (outgoing) quasiparticle state defined by trajectory $\hat{\mathbf{p}}(\hat{\mathbf{p}})$, then the boundary S matrix is a 2×2 spin matrix connecting G and F according to $F = SG$. Translational invariance of the boundary guarantees that only quasiparticles traveling along specular reflected trajectories $\hat{\mathbf{p}}$ and $\hat{\mathbf{p}}$ are related. As Millis *et al.*⁷ discuss, additional symmetries of the interface further restrict the S matrix. Since the interface considered here does not transmit quasiparticles, the incident current must equal the reflected current, which implies that S is unitary, $SS^\dagger = S^\dagger S = 1$. For a magnetically active interface, the general form of the 2×2 S matrix is $S = s + \mathbf{m} \cdot \boldsymbol{\sigma}$. In particular, if the boundary is magnetically polarized along the direction $\hat{\boldsymbol{\mu}}$, then $\mathbf{m} \sim \hat{\boldsymbol{\mu}}$.⁹ The general form of S , consistent with the unitarity condition, is

$$S = e^{-i\Phi/2} e^{-i(\Theta/2)\hat{\boldsymbol{\mu}} \cdot \boldsymbol{\sigma}}. \quad (10)$$

Thus, S has the property that it generates rotations in spin space, $S\boldsymbol{\sigma}S^\dagger = \mathbf{R}^{-1}[\Theta\hat{\boldsymbol{\mu}}] \cdot \boldsymbol{\sigma}$, where $\mathbf{R}[\Theta\hat{\boldsymbol{\mu}}]$ rotates a spin vector about $\hat{\boldsymbol{\mu}}$ by the angle Θ . The S matrix also introduces an overall phase factor, Φ , between the incident and reflected states; however, this phase does not enter the QC boundary condition, so we drop it from here on. The angle Θ that parametrizes the S matrix has the simple interpretation as the spin mixing angle. In particular, assume the boundary magnetization is polarized along the $\hat{\mathbf{y}}$ direction as shown in Fig. 1, and consider an incident quasiparticle with its spin aligned along the $+\hat{\mathbf{z}}$ axis ($G = |\sigma_z = +\rangle$). The outgoing quasiparticle amplitude is a superposition of states with $\sigma_z = \pm 1$ given by $F = \cos(\Theta/2)|+\rangle + \sin(\Theta/2)|-\rangle$. Thus the spin is rotated by its interaction with the internal field of the boundary. This spin rotation occurs only as a result of a tunneling by the quasiparticle into the classically forbidden region of the boundary.

The spin mixing angle Θ depends on the conserved momentum parallel to the surface. Thus for a metal with

a spherical Fermi surface, Θ depends on $(\hat{\mathbf{p}})_\parallel = \hat{\mathbf{p}} - (\hat{\mathbf{p}} \cdot \hat{\mathbf{z}})\hat{\mathbf{z}}$. Quite generally we expect quasiparticles with trajectories that just graze the surface to exhibit the smallest spin rotation upon reflection. An explicit form for the dependence of Θ on the conserved momentum may be obtained from a microscopic model of the magnetic boundary; we provide such a model in the Appendix. However, Θ is perhaps best regarded as a material parameter to be derived from experiment, although one expects that the microscopic model will provide some information on the qualitative dependence on $(\hat{\mathbf{p}})_\parallel$ and the order of magnitude of Θ . It is important to note that the S matrix given in Eq. (10) assumes the magnetic boundary is adequately represented by a potential that couples to the conduction electrons at the surface. The S matrix does not describe dynamical spin-flip interactions between conduction electrons that tunnel into the insulator and local moments in the boundary. However, it does represent, and this is the particular model we discuss in the Appendix, the interaction of the conduction electrons with the mean exchange field, or the magnetization if relevant, of the magnetic ions in the insulator.

The BC connecting the QC propagators for momentum directions related by specular reflection (i.e., $\hat{\mathbf{p}}$ and $\hat{\mathbf{p}}$ in Fig. 1) takes the form of a unitary transformation between $\hat{\mathbf{g}}(\hat{\mathbf{p}}, \mathbf{R}; \epsilon_b)$ and $\hat{\mathbf{g}}(\hat{\mathbf{p}}, \mathbf{R}; \epsilon_n)$ at the surface,⁷

$$\hat{\mathbf{g}}(\hat{\mathbf{p}}, \mathbf{R}_{\text{surface}}; \epsilon_n) = \hat{\mathbf{S}} \hat{\mathbf{g}}(\hat{\mathbf{p}}, \mathbf{R}_{\text{surface}}; \epsilon_b) \hat{\mathbf{S}}^\dagger, \quad (11)$$

where the 4×4 matrix $\hat{\mathbf{S}}$ is simply related to the 2×2 spin matrix S . In particle-hole space

$$\hat{\mathbf{S}} = \begin{bmatrix} S(\hat{\mathbf{p}}, \hat{\boldsymbol{\mu}}) & 0 \\ 0 & S^*(-\hat{\mathbf{p}}, -\hat{\boldsymbol{\mu}}) \end{bmatrix} = \begin{bmatrix} e^{-i(\Theta/2)\hat{\boldsymbol{\mu}} \cdot \boldsymbol{\sigma}} & \\ 0 & e^{-i(\Theta/2)\hat{\boldsymbol{\mu}} \cdot \boldsymbol{\sigma}^{\text{tr}}} \end{bmatrix}. \quad (12)$$

The bottom right-hand element of $\hat{\mathbf{S}}$ is the S matrix for quasiholes reflecting from the boundary. Quasihole states are constructed from quasiparticle states by complex conjugation; this operation reverses the direction of propagation $\hat{\mathbf{p}}$, and for magnetic surfaces the quasiholes experience a magnetic surface potential obtained by $\hat{\boldsymbol{\mu}} \rightarrow -\hat{\boldsymbol{\mu}}$, which accounts for the relation between the quasihole S matrix and the quasiparticle S matrix. These differences in the scattering amplitudes for normal-state quasiparticles and quasiholes are particularly important for a description of the elementary excitations in the superconducting phase interacting with the magnetic surface, because these excitations of the superconductor are superpositions of normal-state quasiparticle and quasihole states.

IV. BULK SUPERCONDUCTOR BOUNDED BY A MAGNETIC WALL

We first consider a superconductor occupying the half-space $z > 0$, bounded by a magnetic wall at $z = 0$. The wall is assumed translationally invariant in the x - y plane, so that the QC differential equation is effectively one dimensional (we do not consider broken translational sym-

metry states near the surface). We introduce dimensionless units by scaling energies in units of T_{c0} , the bulk superconducting transition temperature, and lengths in units of the zero-temperature coherence length, $\xi_0 \equiv \hbar v_F / 2\pi k_B T_{c0}$. In terms of the trajectory coordinate,

$$s = \frac{z}{\frac{v_F}{T_{c0}}(\hat{\mathbf{p}} \cdot \hat{\mathbf{z}})} = \frac{z}{2\pi\xi_0(\hat{\mathbf{p}} \cdot \hat{\mathbf{z}})}, \quad (13)$$

the QC differential equation (neglecting Fermi liquid effects for the present discussion) becomes,

$$[i\epsilon_n \hat{\tau}_3 + \hat{\Delta}, \hat{\mathbf{g}}] + i\partial_s \hat{\mathbf{g}} = 0. \quad (14)$$

Since $z \geq 0$, s has the sign of $\hat{\mathbf{p}} \cdot \hat{\mathbf{z}}$, and extends from $-\infty$ to 0 for $\hat{\mathbf{p}} \cdot \hat{\mathbf{z}} < 0$, and from 0 to $+\infty$ for $\hat{\mathbf{p}} \cdot \hat{\mathbf{z}} > 0$. The propagators for the trajectory $\hat{\mathbf{p}}$ and its specular reflected partner $\hat{\mathbf{p}}$ are connected by the BC at $z=0$ [Eq. (11)]. Thus we can calculate $\hat{\mathbf{g}}(\hat{\mathbf{p}}, z; \epsilon_n)$ and $\hat{\mathbf{g}}(\hat{\mathbf{p}}, z; \epsilon_n)$ by defining

$$\hat{\mathbf{g}}(s; \epsilon_n) = \begin{cases} \hat{\mathbf{g}}(\hat{\mathbf{p}}, z; \epsilon_n), & s > 0 \\ \hat{\mathbf{g}}(\hat{\mathbf{p}}, z; \epsilon_n), & s < 0, \end{cases} \quad (15)$$

where we choose $\hat{\mathbf{p}} \cdot \hat{\mathbf{z}} > 0$, and solving the differential equation (14) in the full space $-\infty < s < \infty$ subject to the BC of Eq. (11) for $s=0$. In addition, the physical solution must satisfy the asymptotic condition

$$\lim_{|s| \rightarrow \infty} \hat{\mathbf{g}}(s; \epsilon_n) = \hat{\mathbf{g}}_b = \frac{i\epsilon_n \hat{\tau}_3 - \hat{\Delta}_b}{(\epsilon_n^2 + \Delta_b^2)^{1/2}}, \quad (16)$$

where Δ_b is the bulk equilibrium gap at the specified temperature.

We solve Eqs. (11)–(16) numerically on a computer. Care must be taken to obtain the physical solution of Eq. (14) since this equation has exponentially exploding solutions in addition to the physical solution that is bounded everywhere. Numerical integration of Eq. (14) is unstable, since even a tiny admixture of the exponentially exploding solution will always dominate the bounded solution. However, we construct the physical solution of Eq. (14) by implementing the observation of Thuneberg *et al.*,¹⁰ that the physical solution can be constructed as

$$\hat{\mathbf{g}}(s, \epsilon_n) \sim [\hat{\mathbf{g}}_+(s, \epsilon_n), \hat{\mathbf{g}}_-(s, \epsilon_n)]_-, \quad (17)$$

where $\hat{\mathbf{g}}_{\pm}(s, \epsilon_n)$ is the exploding solution for $s \rightarrow \pm\infty$. The overall normalization is fixed by the asymptotic boundary condition. The solutions $\hat{\mathbf{g}}_{\pm}(s, \epsilon_n)$ are easily computed numerically by starting the integration at some large value of $|s|$, where the solution is fixed by the bulk gap, and integrating forward (backward) to obtain $\hat{\mathbf{g}}_+(s)[\hat{\mathbf{g}}_-(s)]$. It is important to note that the magnetic boundary condition on the physical solution $\hat{\mathbf{g}}(s, \epsilon_n)$ at $s=0$ is satisfied simply by imposing the BC in Eq. (11) on the unphysical solutions $\hat{\mathbf{g}}_{\pm}(s, \epsilon_n)$. Finally, to complete the half-space solution for $\hat{\mathbf{g}}(\hat{\mathbf{p}}, z; \epsilon_n)$ we must solve Eq. (14) with the self-consistently determined gap $\hat{\Delta}(z)$. This self-consistency requirement is implemented by a Newton iteration procedure to update $\hat{\Delta}(z)$ after $\hat{\mathbf{g}}(\hat{\mathbf{p}}, z; \epsilon_n)$ has

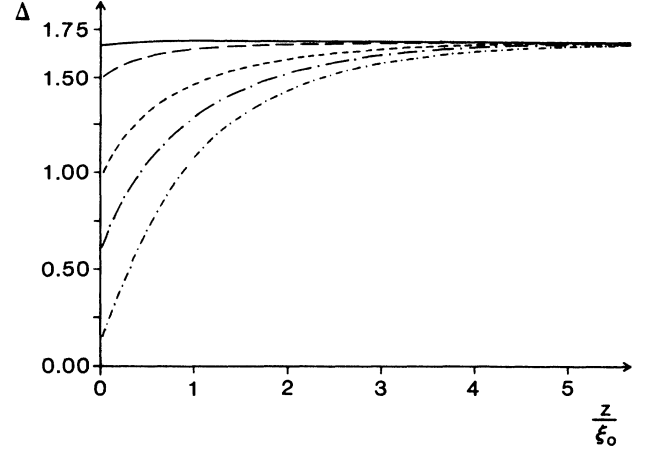


FIG. 2. The normalized order parameter Δ in units of T_{c0} as a function of distance z/ξ_0 from the magnetic insulator. The different curves correspond to $\Delta(z)$ for several values of the spin mixing angle Θ : $\Theta=0.2$ (solid), 0.6 (long-dash), 1.20 (short dash), $\pi/2$ (long dash-dot), and $3\pi/4$ (short dash-dot).

been computed.¹¹

Figure 2 shows the suppression of the gap function $\Delta(z)$ in the vicinity of the magnetic surface. The gap at the surface $\Delta(z=0)$ decreases monotonically as Θ increases from zero, and as the spin mixing angle $\Theta \rightarrow \pi$ the gap $\Delta(z=0) \rightarrow 0$. As expected $\Delta(z)$ heals to the bulk equilibrium gap on the length scale ξ_0 . Figure 3 shows the exchange field [Eq. (8)] induced in the superconductor by the magnetic boundary. The exchange field extends a distance of order ξ_0 into the superconductor, with the penetration depth increasing slightly with increasing Θ . Note that the induced field at the wall passes through a maximum as Θ increases. Such a maximum occurs because at sufficiently large Θ the magnetic surface scattering destroys the superconductivity at the wall, forcing the exchange field to vanish at $z=0$.

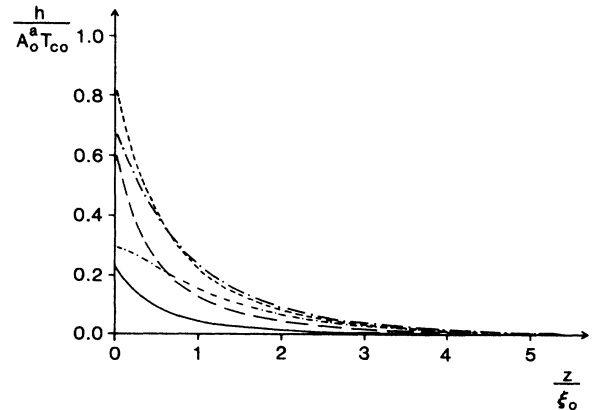


FIG. 3. The induced exchange field in the superconductor, in units of $A_0 T_{c0}$, as a function of distance into the superconductor. The different curves correspond to the same values of Θ given for Fig. 2.

V. THIN SUPERCONDUCTING FILM BACKED BY A MAGNETIC WALL

We now specialize to the thin-film geometry shown in Fig. 1, in which the thin superconducting film of thickness d is sandwiched between a magnetic insulator (a perfectly reflecting magnetic wall) and a perfectly reflecting nonmagnetic surface. This geometry was used by Tedrow *et al.*³ for their tunneling measurements on EuO/Al/Al₂O₃ films. Of course the oxide barrier, Al₂O₃, is weakly transparent, but to a good approximation we may assume it is perfectly reflecting. The walls are also assumed to be translationally invariant in the x - y plane, and for simplicity we assume the internal field of the magnetic insulator is along the \hat{y} direction. Furthermore, the thickness of the film d is assumed small compared to the coherence length, $\xi_0 = \hbar v_F / 2\pi k_B T_c$; the gap Δ is then taken as constant. The transport equation becomes

$$[\hat{\mathbf{M}}, \hat{\mathbf{g}}]_- + iv_F (\hat{\mathbf{p}} \cdot \hat{\mathbf{z}}) \partial_z \hat{\mathbf{g}}(\hat{\mathbf{p}}, z; \epsilon_n) = 0, \quad (18)$$

where $\hat{\mathbf{M}} = i\epsilon_n \hat{\tau}_3 - \hat{\Delta}$.

For the nonmagnetic surface at $z=d$, the propagator is continuous along the classical trajectory defined by $\hat{\mathbf{p}}$ and its specular reflected partner $\hat{\mathbf{p}}$,

$$\hat{\mathbf{g}}(\hat{\mathbf{p}}, d) = \hat{\mathbf{g}}(\hat{\mathbf{p}}, d). \quad (19)$$

For the magnetic wall at $z=0$, we have from Eq. (12),

$$\hat{\mathbf{g}}(\hat{\mathbf{p}}, 0) = \hat{\mathbf{S}} \hat{\mathbf{g}}(\hat{\mathbf{p}}, 0) \hat{\mathbf{S}}^\dagger, \quad (20)$$

where $\hat{\mathbf{S}} = \cos(\Theta/2) - i \sin(\Theta/2) \sigma_2 \tau_3$, and by convention we take $\hat{\mathbf{p}} \cdot \hat{\mathbf{z}} > 0$, $\hat{\mathbf{p}} = \hat{\mathbf{p}} - 2\hat{\mathbf{z}}(\hat{\mathbf{p}} \cdot \hat{\mathbf{z}})$. Equations (18)–(20) are solved in the thin-film limit, $d \ll \xi_0$, with the *ansatz*

$$\hat{\mathbf{g}}(\hat{\mathbf{p}}, z) = \hat{\mathbf{g}}_0(\hat{\mathbf{p}}) + (z-d)\hat{\mathbf{g}}_1(\hat{\mathbf{p}}), \quad (21)$$

with $\hat{\mathbf{g}}_0$ and $\hat{\mathbf{g}}_1$ independent of z , and $\|d\hat{\mathbf{g}}_1\| \ll \|\hat{\mathbf{g}}_0\|$.¹²

The boundary condition at the nonmagnetic wall ($z=d$) implies

$$\hat{\mathbf{g}}_0(\hat{\mathbf{p}}) = \hat{\mathbf{g}}_0(\hat{\mathbf{p}}), \quad (22)$$

and together with the two transport equations for $\hat{\mathbf{g}}(\hat{\mathbf{p}})$, this implies

$$\hat{\mathbf{g}}_1(\hat{\mathbf{p}}) = -\hat{\mathbf{g}}_1(\hat{\mathbf{p}}). \quad (23)$$

The boundary condition at $z=0$ is then equivalent to

$$[\hat{\mathbf{g}}_0(\hat{\mathbf{p}}), \hat{\mathbf{S}}]_- = d [\hat{\mathbf{g}}_1(\hat{\mathbf{p}}), \hat{\mathbf{S}}]_+. \quad (24)$$

By taking the anticommutator of the transport equation (18) with $\hat{\mathbf{S}}$, we eliminate $\hat{\mathbf{g}}_1(\hat{\mathbf{p}})$ to obtain the following equation for $\hat{\mathbf{g}}_0$:

$$[[\hat{\mathbf{M}}, \hat{\mathbf{g}}_0]_-, \hat{\mathbf{S}}]_+ + \frac{iv_F |\hat{\mathbf{p}} \cdot \hat{\mathbf{z}}|}{d} [\hat{\mathbf{g}}_0, \hat{\mathbf{S}}]_- = 0. \quad (25)$$

Using the explicit form for $\hat{\mathbf{S}}$ from Eq. (12), we obtain

$$\begin{aligned} [\hat{\mathbf{M}}, \hat{\mathbf{g}}_0]_- - \frac{i}{2} \tan(\Theta/2) [[\hat{\mathbf{M}}, \hat{\mathbf{g}}_0]_-, \hat{\mathbf{S}}]_+ \\ + \frac{v_F |\hat{\mathbf{p}}_z|}{2d} \tan(\Theta/2) [\hat{\mathbf{g}}_0, \hat{\mathbf{S}}]_- = 0, \end{aligned} \quad (26)$$

where $\hat{\mathbf{S}} = \sigma_x \tau_3$.

Equation (26) and the normalization condition suggest that $\hat{\mathbf{g}}_0$ is of the form

$$\hat{\mathbf{g}}_0 = A (\hat{\mathbf{M}} - \alpha \hat{\mathbf{S}}) + B \sigma_2 (\hat{\mathbf{M}} - \alpha \hat{\mathbf{S}}). \quad (27)$$

We then obtain the solution for $\hat{\mathbf{g}}_0$ with

$$\begin{aligned} \alpha &= \frac{v_F |\hat{\mathbf{p}}_z|}{2d} \tan\left(\frac{\Theta}{2}\right), \\ A \pm B &= -\pi \left[\frac{1}{\beta \pm 2i\epsilon_n \alpha} \right]^{1/2}, \end{aligned} \quad (28)$$

where

$$\beta = \epsilon_n^2 + \Delta^2 - \alpha^2. \quad (29)$$

We discuss some of the properties of this solution in Secs. VI and VII.

VI. PAIRBREAKING EFFECT ON T_c AND Δ

Magnetic scattering by a boundary is destructive to conventional spin-singlet superconductivity. The gap parameter Δ is suppressed near a magnetic surface; for very strong pair-breaking Δ is forced to zero at the magnetic wall. For the half-space model described in Sec. IV, $\Delta(z=0) = 0$ in the extreme limit in which the spin mixing angle $\Theta = \pi$ (for all $\hat{\mathbf{p}}$). In this limit an electron with trajectory $\hat{\mathbf{p}}$ and spin projection $\sigma_z = +1$ is reflected into the trajectory $\hat{\mathbf{p}}$ and spin projection $\sigma_z = -1$ with unit probability. The wall is then a perfect pair breaker; it is simple to show that if $\Theta = \pi$, then only solutions for $\hat{\mathbf{g}}$ with $\Delta = 0$ at the wall satisfy the transport equation and boundary conditions. This limit of perfect pair breaking is the boundary condition often employed in phenomenological Ginsburg-Landau theories of magnetic and superconducting proximity contacts formed from strong ferromagnetic materials like Fe, Gd, Ni, etc.^{1,13} However, the more interesting limit occurs for $\Theta < \pi$, in fact for $\Theta \ll 1$, in which case the magnetic boundary is not capable of completely destroying superconductivity at the interface. This limit is relevant for rare-earth-oxide magnets in proximity contact with superconductors.^{3,14}

The pair-breaking effect of the boundary magnetism on the gap and T_c can be calculated from the weak-coupling gap equation obtained from Eqs. (3) and (27)–(29),

$$\frac{1}{v_0} = \frac{\pi}{\sqrt{2}} \int \frac{d\Omega}{4\pi} T \sum_n \left[\frac{[\beta + (\beta^2 + 4\epsilon_n^2 \alpha^2)^{1/2}]^{1/2}}{(\beta^2 + 4\epsilon_n^2 \alpha^2)^{1/2}} \right]. \quad (30)$$

In the limit $\alpha \rightarrow 0$ (i.e., no magnetic scattering), we obtain the standard BCS gap equation,

$$\frac{1}{v_0} = \int \frac{d\Omega}{4\pi} T \sum_n \frac{\pi}{(\epsilon_n^2 + \Delta^2)^{1/2}}. \quad (31)$$

This is the well-known result that specular reflection from a nonmagnetic wall is not pair breaking for conventional s -wave superconductivity. Since the frequency sum is logarithmically divergent and must be cut off at a high frequency $\Omega_{\text{Debye}} \gg 2\pi T_c$, we eliminate the unphysical cutoff and the pairing interaction in favor of the bulk

transition temperature T_{c0} of the clean superconductor in the standard way, by defining,

$$K(T) = \pi T \sum_n \frac{|\epsilon_n| < \Omega_{\text{Debye}}}{|\epsilon_n|} \simeq \ln(1.13 \Omega_{\text{Debye}}/T). \quad (32)$$

We thus have $1/v_0 = K(T_{c0})$, and the gap equation defining Δ for the thin film in contact with the magnetic boundary can now be linearized to obtain an equation for T_c of the film in terms of T_{c0} and the magnetic surface pair-breaking parameter α ,

$$\ln(T_c/T_{c0}) = -\pi T_c \sum_n \int_0^1 du \frac{\alpha(u)^2}{|\epsilon_n| [\epsilon_n^2 + \alpha(u)^2]}, \quad (33)$$

where $\alpha(u) = v_F/2d |u| \tan[\Theta(u)/2]$. In general, the spin mixing angle $\Theta(u)$ depends on $u = (\hat{z} \cdot \hat{p})$. However, assuming Θ is constant, we obtain the following equation for $T_c/T_{c0} = t$:

$$\ln(t) = -f(t/\rho),$$

$$f(y) = \sum_{n \geq 0} \left[\frac{1}{(n + \frac{1}{2})} \right] \times \left[1 - (n + \frac{1}{2})y \tan^{-1} \left[\frac{1}{y(n + \frac{1}{2})} \right] \right], \quad (34)$$

$$\rho = \left[\frac{v_F \tan \left[\frac{\Theta}{2} \right]}{4\pi d T_{c0}} \right].$$

The dimensionless surface pair-breaking parameter is $\rho = \xi_0/2d \tan(\Theta/2)$; thus even if $\Theta \ll 1$, ρ need not be small since we have assumed $\xi_0 \gg d$. Nevertheless for small $\rho \ll 1$ we obtain

$$T_c/T_{c0} \simeq 1 - \frac{7\zeta(3)}{3} \rho^2. \quad (35)$$

Thus, for fixed magnetic-surface scattering the transition temperature of the film decreases with the film thickness as $(T_{c0} - T_c)/T_{c0} \sim (\xi_0/d)^2$. Equation (35) also suggests that magnetic-surface pair breaking is capable of destroying superconductivity in thin films ($d \ll \xi_0$) even if the spin mixing angle $\Theta \ll 1$. As shown in Fig. 4, T_c is suppressed to zero as ρ approaches a critical value ρ_c , which can be calculated from Eq. (33) in the limit $\rho/T_c(\rho) \rightarrow \infty$. For an interface with $\Theta(u)$ independent of u ,

$$\rho_c = \exp[1 + \psi(\frac{1}{2})] \simeq 0.3816,$$

where $\psi(x)$ is the digamma function.

The effect of magnetic scattering on the gap can be calculated from Eq. (30). The zero-temperature gap as a function of ρ is shown as the insert of Fig. 4, and follows qualitatively the form of $T_c(\rho)$.¹⁵ The temperature dependence of the gap also changes as a result of magnetic surface scattering. Figure 5 shows the deviation of the scaled gap $\Delta(\rho, T)/\Delta(\rho, 0)$ from the universal BCS gap function $\Delta_{\text{BCS}}(T)/\Delta_{\text{BCS}}(0)$.

In the Ginsburg-Landau region, $\Delta(\rho, T)/T_c(\rho) \ll 1$,

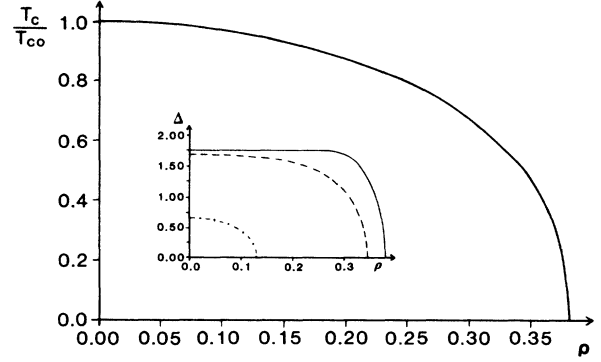


FIG. 4. The transition temperature of a pure superconducting film as a function of the magnetic surface pairbreaking parameter ρ . The inset shows the temperature-dependent gap function $\Delta(\rho, T)/T_{c0}$ for temperatures $T/T_{c0} = 0.5$ (solid), 0.5 (dash), and 0.95 (dash-dot).

the temperature dependence of $\Delta(T)$ retains the conventional mean-field form,

$$\Delta(T, \rho) = G(\rho) T_c(\rho) [1 - T/T_c(\rho)]^{1/2}, \quad (36)$$

where $G(\rho)$ increases from the BCS value of $G(0) = 3.06$ to $G(0.8\rho_c) = 3.47$. Finally, we conclude this section with a discussion of the order of the phase transition in a thin superconducting film in contact with a magnetic insulator. It is well known that the order of the phase transition in a thin superconducting film in an external magnetic field depends upon the temperature, as well as the purity of the metal. Sarma¹⁶ and Maki and Tsunto¹⁷ showed that the superconducting transition is first order for temperatures below $0.56T_c$, with critical field at $T=0$ given by the Chandrasekhar-Clogston limiting field $\mu_e H_c(0) = \Delta(0)/\sqrt{2}$; at temperatures $T > 0.56T_c$ the transition is second order.¹⁸ For a superconducting film in contact with a magnetic insulator, the magnetic-surface pair-breaking parameter, $\alpha = v_F/2d |\hat{p} \cdot \hat{z}| \tan(\Theta/2)$, plays a role similar to an external magnetic field. In fact,

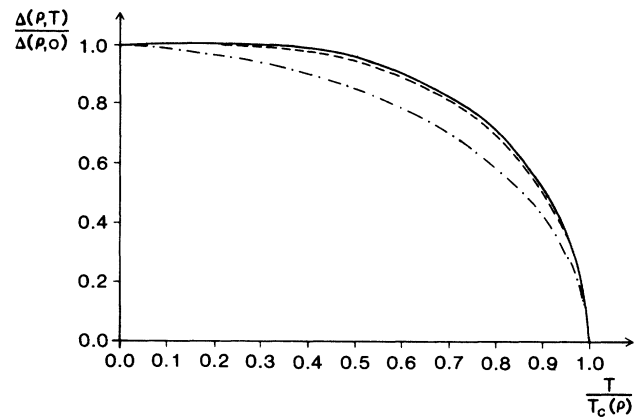


FIG. 5. The normalized gap $\Delta(T, \rho)/\Delta(0, \rho)$ as a function of reduced temperature $T/T_c(\rho)$, for $\rho=0$ (solid), 0.1 (dash), 0.38 (dash-dot).

the QC transport equation [Eq. (26)] for the propagator $\hat{\mathbf{g}}_0$ has precisely the same form as the QC transport equation for a bulk, homogeneous superconductor interacting with a uniform field $\alpha\hat{\mathbf{y}}$, *only* via the quasiparticle electron spin. We might, therefore, expect the transition from the superconducting to the normal state to be first-order at low temperatures provided the surface pair-breaking field α was sufficiently large. This turns out not to be the case; in zero external field the transition is always second order, independent of the strength of the surface pair-breaking field α . The reason that a superconducting film which is in contact with a magnetic insulator differs from a thin superconducting film in an external field is that the surface pair-breaking field α depends upon the quasiparticle trajectory; in particular $\alpha \rightarrow 0$ as $|\hat{\mathbf{p}} \cdot \hat{\mathbf{z}}| \rightarrow 0$. Thus there is always a set of trajectories for which the surface pair-breaking field is relatively weak. This dependence of $\alpha(u)$ on $u = \hat{\mathbf{p}} \cdot \hat{\mathbf{z}}$ leads to a softening of the transition to second order even at $T=0$. We demonstrate this fact by considering the Ginzburg-Landau (GL) region in which the gap function Δ is presumed small. The GL free-energy functional has the conventional form

$$\Delta\Omega[\Delta] = a(T, \rho)\Delta^2 + \frac{1}{2}b(T, \rho)\Delta^4 + \dots \quad (37)$$

The gap parameter becomes

$$\Delta^2 = -a(T, \rho)/b(T, \rho), \quad (38)$$

where $a(T, \rho)$ and $b(T, \rho)$ are the GL coefficients for a thin film in contact with a magnetic insulator. This result presumes the transition is second order, and therefore that the coefficient $b(T, \rho) > 0$. Otherwise, if $b(T, \rho) < 0$ the fourth-order GL functional does not have a stable minimum and consequently the sixth-order term which stabilizes the minimum of $\Delta\Omega$ also forces the transition to be first order. We calculate $b(T, \rho)$ from the expansion of the gap equation to third order in Δ ; the result is

$$b = \frac{\pi T}{2} \sum_{n \geq 0} \int_{-1}^1 du \operatorname{Re} \left[\frac{1}{\epsilon_n + i\alpha} \right]^3. \quad (39)$$

For a constant *external* magnetic field we set $\alpha = \mu_e H$ (independent of u), so that

$$b_{\text{ext}} = \pi T \sum_{n \geq 0} \frac{\epsilon_n^3 - 3\epsilon_n(\mu_e H)^2}{[\epsilon_n^2 + (\mu_e H)^2]^3}. \quad (40)$$

Thus for an external magnetic field the fourth-order coefficient is negative for sufficiently low temperature and high field, thus signaling a first-order transition.

However, for $\alpha = \alpha_0 |u|$, appropriate for a magnetic-superconducting proximity contact, we find

$$b_{\text{prox}} = \pi T \sum_{n \geq 0} \frac{\epsilon_n}{(\epsilon_n^2 + \alpha_0^2)^2}, \quad (41)$$

which is strictly positive, thus implying a second-order transition for any temperature and surface pair-breaking parameter $\alpha_0 = v_F/2d \tan\Theta_0$.

VII. INTERNAL FIELD, FERMI-LIQUID EFFECTS, AND THE DENSITY OF STATES

In addition to pair-breaking effects, scattering of quasiparticles by a magnetic surface polarizes the superconducting film. This polarization is responsible for the induced exchange field discussed earlier for the half-space superconductor. For a thin superconducting film the polarization may be inferred from Eq. (26) for the propagator $\hat{\mathbf{g}}_0$, which, as mentioned before, has the same form as the QC transport equation for a bulk, homogeneous superconductor interacting with a uniform magnetic field $\alpha\hat{\mathbf{y}}$, *only* via the quasiparticle electron spin.

In addition to the field $\alpha\hat{\mathbf{y}}$ resulting from electrons tunneling into the insulating magnet, there is an exchange field induced in the superconductor which is calculated from Eq. (8), and is shown in Fig. 6 as a function of ρ for $T/T_{c0} = 0.5$, or equivalently the average effective field $\bar{\alpha} = (2\pi/3)T_{c0}\rho$. For small $\bar{\alpha}$ the exchange field is linear in $\bar{\alpha}$,

$$h = \left[\frac{F_0^a(1-y)}{1+yF_0^a} \right] \bar{\alpha}, \quad (42)$$

where $F_0^a = A_0^a/(1-A_0^a)$ is the Fermi-liquid parameter representing the exchange interaction of the metal, and y is the Yoshida function,

$$1-y = \pi T \sum_n \frac{\Delta^2}{(\epsilon_n^2 + \Delta^2)^{3/2}}. \quad (43)$$

Near the transition temperature ($T \simeq T_c \simeq T_{c0}$) the exchange field

$$h \simeq \left[\frac{F_0^a}{1+F_0^a} \right] \left[\frac{7\zeta(3)}{4\pi^2} \frac{\Delta^2}{T_c^2} \right] \bar{\alpha}, \quad (44)$$

is small; however, at low temperatures,

$$h \simeq F_0^a \bar{\alpha}, \quad (45)$$

which may be comparable to the field $\bar{\alpha}$ if the Fermi-liquid exchange interaction parameter F_0^a is sizable.

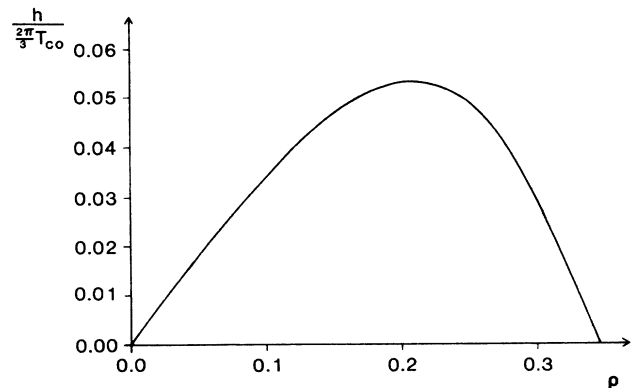


FIG. 6. The exchange field, calculated self-consistently, for a thin film in contact with a magnetic insulator is shown as a function of ρ , for $A_0^a = 0.23$ (representative of Al) $T/T_{c0} = 0.5$.

Tedrow *et al.*¹⁹ have determined F_0^a using spin-polarized tunneling techniques in Al films and find $F_0^a \simeq 0.3$ to 0.4. This Fermi-liquid effect should be included in making quantitative comparisons with tunneling data to extract, for instance, the parameter α . Finally, for large values of ρ the exchange field is no longer linear in $\bar{\alpha}$, and in fact vanishes as $\rho \rightarrow \rho_c$ (see Fig. 6).

The field α has an important effect on the DOS of the superconducting film; a spin-splitting of the DOS results from the tunneling of electrons into the polarized insulator. We calculate the DOS of the film in the standard way by analytically continuing the Matsubara propagator to the real axis to obtain the retarded (R) propagator according to $g^R(E) = g_0(i\epsilon_n \rightarrow E + i\eta)$, where g_0 represents the upper left 2×2 matrix (in particle-hole space) of \hat{g}_0 . Choosing $\hat{\mu}$ as the quantization axis diagonalizes g_0 , with diagonal elements g_{\pm} for the two spin bands. The resulting angle-resolved DOS, calculated from

$$N_{\sigma}(\hat{\mathbf{p}}, E) = -\frac{N(0)}{\pi} \text{Im}[g_{\sigma}^R(\hat{\mathbf{p}}, E)]; \quad \sigma = \pm, \quad (46)$$

is shown in Fig. 7. Each curve has essentially the form of a BCS square-root singularity. For the spin-up ($\sigma = +$) band displaced highest in energy,

$$N_{+}(\hat{\mathbf{p}}, E) = N(0) \frac{E - \alpha}{[E + (\Delta - \alpha)][E - (\Delta + \alpha)]}, \quad (47)$$

where $N(0)$ is the DOS in the normal metal.

The angle-resolved DOS depends on the trajectory $\hat{\mathbf{p}}$, through the surface field $\alpha \sim |\hat{\mathbf{p}} \cdot \hat{\mathbf{z}}|$. Indeed for quasiparticle trajectories grazing the interface there is no spin-splitting at all if we neglect Fermi-liquid effects. To include Fermi-liquid effects, as well as an applied field \mathbf{H} parallel to the interface (which we assume will orient the internal field of the insulator parallel to \mathbf{H}), we replace α by $\alpha + h_{\text{ext}} + h$, where $h_{\text{ext}} = \mu_e H$ is the external field, and h is the exchange field [Eq. (8)] of the metal film resulting from both α and h_{ext} .²⁰ In this case even the DOS for quasiparticles with trajectories nearly parallel to the surface will exhibit a spin-splitting given by the field $(h_{\text{ext}} + h)$. Nevertheless, the maximum spin-splitting

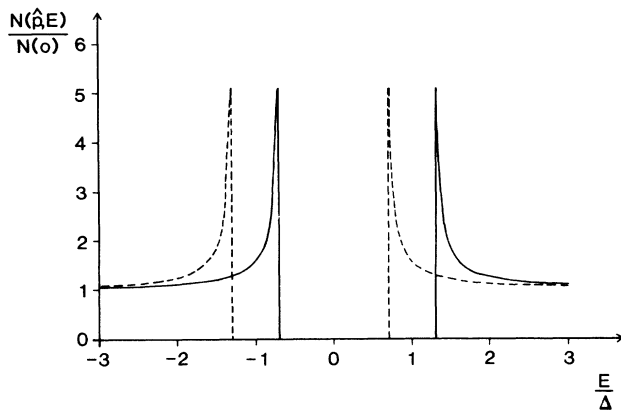


FIG. 7. The spin-resolved density of states as a function of energy E/Δ measured from the Fermi level. The figure assumes the internal field of the insulator to be $\alpha_0 = 0.3\Delta$.

occurs for quasiparticles following trajectories that are normal to the interface. This is also the spin-splitting that will be observed in a tunneling measurement of the DOS because the tunneling matrix element falls off exponentially with the oxide barrier thickness; thus, any tunneling measurement will preferentially select quasiparticles moving perpendicular to the interface.

Finally, we note that the magnetic surface does not influence the DOS of the normal metal [see Eq. (47)]. The film is essentially bulk metal for $d \gg k_F^{-1}$, and is well described by bulk metal quasiparticles; so long as $\alpha \ll E_F$, the normal state DOS is unchanged, to high accuracy, by magnetic surface scattering.

VIII. EuO/Al/Al₂O₃/ELECTRODE TUNNEL JUNCTIONS

Tedrow *et al.*³ recently measured the tunneling conductance of thin ($d \ll \xi_0$) superconducting Al films in contact with films of EuO, which in bulk form is a ferromagnetic semiconductor with a Curie temperature of 70 K and an optical band gap of 1.1 eV.⁴ The tunneling conductances of these junctions show a spin splitting of the Al DOS in excess of the splitting observed for Al films in contact with nonmagnetic substrates. In particular, the spin-splitting between adjacent peaks in the DOS—as inferred from the tunneling conductance—is $2\mu_e(H + B^*)$, where H is the applied field (aligned parallel to the EuO/Al interface) and B^* represents the excess spin splitting. In a field $H = 0.44$ T Tedrow *et al.* find $B^* = 1.73$ T for an Al film 40 Å thick in contact with approximately 50 Å of EuO. The excess spin splitting is field dependent, vanishing at $H = 0$ and saturating at $B^* \simeq 2.0$ T for $H \geq 0.8$ T. The fact that $B^*(H = 0) = 0$ implies that the EuO is not ferromagnetically ordered in the proximity contact even though the operating temperature, $T \simeq 0.4$ K, is 2 orders of magnitude below the Curie temperature of bulk EuO. Thus there is a strong effect on the magnetic properties of the EuO film when prepared in the EuO/Al proximity contact. Below we relate the excess splitting B^* to the average exchange field, produced by the aligned Eu²⁺ moments, acting on the Al conduction electrons that tunnel into the insulator.

Tedrow *et al.* interpret the excess spin splitting B^* in terms of a coupling between the Al conduction electrons and the EuO magnetization. In particular, they argue that B^* is close in magnitude to the magnetization of EuO measured by Shapira *et al.*,²¹ thus suggesting the coupling of the Al conduction electron magnetic moment to the EuO magnetization. We first consider this possibility in the context of the QC boundary condition and model S matrix discussed in Sec. III and in the Appendix.

If the tunneling electrons, described by Eq. (54), couple only to the magnetization \mathbf{M} of the insulator, then the corresponding internal field of EuO is $\mathbf{h}_i = -4\pi\mu_e\mathbf{M}$. The magnetization of EuO in an external field \mathbf{H} in a mean-field approximation is, $M = M_0 B_J[M; H, T]$, where $M_0 = N_0\mu$ is the saturation magnetization of local moments of total angular momentum J and magnetic moment $\mu = -g(LSJ)\mu_e J$, $B_J[M; H, T]$ is the Brillouin function, and N_0 is the number of moments per unit volume. For Eu²⁺ ions, $J = S = \frac{7}{2}$, and thus we estimate

$M \lesssim M_0 \simeq 0.19$ T at low temperature and high fields.²²

The Zeeman splitting that appears in the Al DOS is calculated from the model for the spin mixing angle Θ ($\Theta=0$) $\equiv \Theta_0$ described in the Appendix. From Eq. (A10) we have

$$\Theta_0 = \frac{2h_i/E_F}{1+(E_g/2E_F)^2}, \quad (48)$$

where $h_i = 4\pi\mu_e M$. With the bulk values for the EuO band gap, $E_g \simeq 1.1$ eV, and the Al Fermi energy of $E_F \simeq 11.7$ eV, we obtain the following estimate for the maximum Zeeman shift in the Al DOS:

$$B^* = \frac{4\pi M}{k_F d} \left(\frac{2E_F}{E_g} \right)^{1/2}, \quad (49)$$

which attains a maximum value of 0.17 T in high fields and low temperatures. This result is a full order of magnitude smaller than the maximum excess splitting observed by Tedrow *et al.* for their EuO/Al film. We have also modified the model interface Hamiltonian [Eq. (54)] to allow for differing carrier effective masses in EuO and Al and find that it is not possible to account for the observed splitting $B^* \simeq 1.7$ T by coupling the tunneling electrons to the EuO magnetization, unless the band gap of EuO in the proximity contact is roughly 2 orders of magnitude smaller than the optical band gap in bulk EuO.

The *exchange coupling* between an itinerant electron and the local moments in EuO typically dominates the coupling to the magnetization. This is certainly the case for a conduction band electron in EuO interacting with the mean exchange field produced by the Eu^{2+} moments. We now consider a model for the interaction between a tunneling electron with the exchange field from the local moments of EuO near the proximity contact. The Hamiltonian is

$$H_{\text{ex}} = \sum_i^{\text{ions}} J_{\text{ex}}(|\mathbf{x}-\mathbf{R}_i|) \mathbf{J}_i \cdot \mathbf{S}_e, \quad (50)$$

where $\mathbf{S}_e = (\hbar/2)\boldsymbol{\sigma}$ is the tunneling electron spin operator, \mathbf{J}_i is the total spin operator of the local moment at position \mathbf{R}_i , and $J_{\text{ex}}(|\mathbf{x}-\mathbf{R}_i|)$ is the exchange potential. In an applied field \mathbf{H} the spin-flip processes described by the above exchange interaction are suppressed, and we replace \mathbf{J}_i by its average value in the field \mathbf{H} , which may be represented as

$$\langle \mathbf{J}_i \rangle = JB_J \left[\frac{\mu H_{\text{tot}}}{k_B T} \right] \hat{\boldsymbol{\mu}}, \quad (51)$$

where $\hat{\boldsymbol{\mu}}$ is the direction of polarization. We also approximate $J_{\text{ex}}(|\mathbf{x}-\mathbf{R}_i|)$ by a constant exchange interaction for \mathbf{x} within the unit cell surrounding the ionic spin at \mathbf{R}_i . The resulting effective Hamiltonian becomes,

$$H_{\text{ex}} \simeq \frac{J}{2} B_J \left[\frac{\mu H_{\text{tot}}}{k_B T} \right] J_{\text{ex}} \hat{\boldsymbol{\mu}} \cdot \boldsymbol{\sigma}, \quad (52)$$

which has the same form considered in the Appendix for obtaining a model S matrix for magnetic scattering at a

perfectly reflecting interface. The exchange interaction for a tunneling electron interacting with local Eu^{2+} ions is not known. However, assuming the exchange interaction J_{ex} in the EuO/Al proximity contact is small compared with the band gap E_g , we can relate the maximum Zeeman shift B_{ex}^* to the maximum exchange field, $h_{\text{ex}} = \frac{7}{4} J_{\text{ex}}$, acting on a tunneling electron,

$$B_{\text{ex}}^* = \left[\frac{h_{\text{ex}}}{\mu_e} \right] \left[\frac{1}{k_F d} \right] \left[\frac{2E_F}{E_g} \right]^{1/2}. \quad (53)$$

Taking $B_{\text{ex}}^* = 1.7$ T from the measurements by Tedrow *et al.*, we infer an exchange field $h_{\text{ex}} \simeq 1.4 \times 10^{-3}$ eV. This exchange energy for a *tunneling* electron interacting with the Eu^{2+} moments at the interface is roughly 2 orders of magnitude smaller than the exchange energy for *band* electrons interacting with Eu^{2+} moments in bulk EuO, as measured by Penney *et al.*²³ Again there is no simple way to account for the observed magnitude of $B^* \simeq 1.7$ T in terms of *bulk* material parameters of EuO and Al; this is not surprising given that EuO is not ferromagnetic in the proximity contact even at temperatures of order 1 K. Clearly, the exchange interaction *between* Eu^{2+} moments is severely reduced by the geometry of the interface and the neighboring metallic environment.

In summary, the observed maximum excess Zeeman splitting $B^* = 1.7$ T in the EuO/Al proximity contacts measured by Tedrow *et al.* cannot be explained in terms of a coupling of the Al tunneling electron spin to the EuO magnetization unless the band gap of EuO in EuO/Al is at least 2 orders of magnitude smaller than the optical gap of 1.1 eV in bulk EuO. However, if we assume that B^* reflects the coupling of the tunneling electrons to the average exchange field of the Eu^{2+} spins at the interface, we obtain an exchange energy of $h_{\text{ex}} \simeq 10^{-3}$ eV. This value is 2 orders of magnitude smaller than the exchange energy of a conduction electron in bulk EuO, and is not necessarily unreasonable given the distinctly different environment for the Eu^{2+} spins in the EuO/Al proximity contact compared to bulk EuO.

ACKNOWLEDGMENTS

We thank Professor J. Kurkijärvi for his critical comments on the boundary condition for the quasiclassical equations. This work was supported by the National Science Foundation under Grant No. DMR 8518163, and through the Northwestern Materials Research Center under Grant No. DMR85-20280.

APPENDIX

Here we calculate the interface scattering matrix $S(E, \mathbf{p}_{\parallel}, \hat{\boldsymbol{\mu}})$ in a model that describes the reflection of electrons, with excitation energy $E \ll E_F$ and conserved momentum parallel to the interface $\hat{\mathbf{p}}_{\parallel}$, incident on a smooth interface between an insulating magnet, with an average internal field \mathbf{h}_i directed along $\hat{\boldsymbol{\mu}}$, and an average band gap E_g .

The Schrödinger equation describing the low-energy electronic states is assumed to be

$$\left[-\frac{1}{2m^*} \nabla^2 + (E_F + \frac{1}{2}E_g + \mathbf{h}_i \cdot \boldsymbol{\sigma}) \theta(-z) \right] \psi = (E + E_F) \psi, \quad (\text{A1})$$

where $(E_g \pm h_i)$ is the bottom of the (empty) conduction band for spin \pm excitations in the insulator ($z < 0$), and E_F is the Fermi level of the metal ($z > 0$). For simplicity first we assume the effective mass m^* is the same for both materials.

The interface is assumed smooth so that

$$\psi = e^{i\mathbf{p}_{\parallel} \cdot \mathbf{x}} \phi(z), \quad (\text{A2})$$

where \mathbf{p}_{\parallel} is the conserved momentum parallel to the interface. The general solution to Eq. (A1) on the metallic side is

$$\psi = (F e^{ipz} + G e^{-ipz}) e^{i\mathbf{p}_{\parallel} \cdot \mathbf{x}}, \quad (\text{A3})$$

where F and G are spinor amplitudes for the "scattering out" and "scattering in" solutions, and $p = |\mathbf{p} \cdot \hat{\mathbf{z}}| = p_F \cos(\vartheta) > 0$. The quantization axis is conveniently chosen to be $\hat{\boldsymbol{\mu}}$, the direction of the internal field of the insulator. Using the notation $\hat{\chi}_{\pm}$ for eigenspinors of $\hat{\boldsymbol{\mu}} \cdot \boldsymbol{\sigma}$ with eigenvalues ± 1 , and F_{\pm} as the corresponding amplitudes of F in this basis, we can match the solutions for $z > 0$ to the physical solution in the insulating region for $E < E_g - h_i$, i.e., excitation energy below the bottom of the lowest band in the insulating region. In this case the allowed solutions for $z < 0$ decay exponentially into the insulator, and electrons incident on the insulator are totally reflected. The solution for $z < 0$ and $E \simeq 0$ (i.e., electrons on the Fermi surface) is,

$$\psi_{\pm}(\mathbf{x}) = A_{\pm} e^{q_{\pm} z} e^{i\mathbf{p}_{\parallel} \cdot \mathbf{x}}, \quad (\text{A4})$$

$$q_{\pm} = [p_F^2 \sin^2(\vartheta) + 2m^*(E_g \pm h_i)]^{1/2}, \quad (\text{A5})$$

and $|\mathbf{p}_{\parallel}| = p_F \sin(\vartheta)$. Note that the decay lengths q_{\pm}^{-1} differ most for normal incidence ($\vartheta=0$); for grazing in-

cidence ($\vartheta \simeq \pm\pi/2$) the decay lengths are $q_{\pm}^{-1} \simeq p_F^{-1} \simeq 1 \text{ \AA}$, which is expected to be short compared to the magnetic penetration length, $(2m^*h_i)^{-1}$, if the energy $h_i \ll E_F, E_g$.

The S -matrix elements are obtained by matching wave functions and derivatives at $z=0$. We then eliminate the amplitudes A_{\pm} to obtain the matrix equation $F = SG$ connecting the "scattering out" amplitude (F) and the "scattering in" amplitude (G); S is diagonal in the $\hat{\chi}_{\pm}$ basis with eigenvalues

$$S_{\pm} = \frac{1 - iq_{\pm}/p}{1 + iq_{\pm}/p}. \quad (\text{A6})$$

It is convenient to express S_{\pm} in terms of the dimensionless parameters $r = (2m^*E_g/p_F)^{1/2}$, $\lambda = h_i/E_g \leq 1$, and the scattering angle $\cos(\vartheta) = |\hat{\mathbf{z}} \cdot \hat{\mathbf{p}}|$:

$$S_{\pm} = \frac{\cos(\vartheta) - i[\sin^2(\vartheta) + r^2(1 \pm \lambda)]^{1/2}}{\cos(\vartheta) + i[\sin^2(\vartheta) + r^2(1 \pm \lambda)]^{1/2}}. \quad (\text{A7})$$

This result is related to Eq. (12) as follows. The upper left (particlelike) 2×2 spin matrix in Eq. (12) is

$$S = e^{-i(\Theta/2)\hat{\boldsymbol{\mu}} \cdot \boldsymbol{\sigma}} = S_+(1 + \hat{\boldsymbol{\mu}} \cdot \boldsymbol{\sigma})/2 + S_-(1 - \hat{\boldsymbol{\mu}} \cdot \boldsymbol{\sigma})/2. \quad (\text{A8})$$

Thus the spin mixing angle Θ depends on the interface parameters (r, λ) and the scattering angle ϑ as

$$\tan \left[\frac{\Theta}{2} \right] = -\frac{2 \text{Im}(S_+ S_-^*)}{|S_+ + S_-|^2}. \quad (\text{A9})$$

For $\lambda \ll 1$ we have $\Theta \ll 1$ and

$$\Theta \simeq \left[\frac{2r^2}{1+r^2} \right] \frac{\cos(\vartheta)}{[\sin^2(\vartheta) + r^2]^{1/2}} \lambda. \quad (\text{A10})$$

For $r \gg 1$, this result further simplifies, $\Theta \simeq 2(\lambda/r) \cos(\vartheta)$, in any case we expect that $\Theta \propto h_i$.

*Current address: Department of Physics and Astronomy, Northwestern University, Evanston, IL 60208.

¹H. K. Wong, B. Y. Jin, H. Q. Yang, J. B. Ketterson, J. E. Hilliard, *Superlatt. Microstructures* **1**, 259 (1985); H. K. Wong and J. B. Ketterson, *J. Low Temp. Phys.* **63**, 139 (1986).

²F. Stageberg, R. Cantor, A. M. Goldman, G. B. Arnold, *Phys. Rev. B* **32**, 3292 (1985); M. J. DeWeert and G. B. Arnold, *Phys. Rev. Lett.* **55**, 1522 (1985).

³P. M. Tedrow, J. E. Tkaczyk, and A. Kumar, *Phys. Rev. Lett.* **56**, 1746 (1986).

⁴The properties of EuO are reviewed by S. Methfessel and D. C. Mattis, *Handbuch der Physik*, edited by S. Flügge (Springer-Verlag, Berlin, 1968), Vol. 18, Pt. 1.

⁵For a recent review of the quasiclassical theory of superconductivity, which includes original references, see J. A. X. Alexander, T. P. Orlando, D. Rainer, and P. M. Tedrow, *Phys. Rev. B* **31**, 5811 (1985).

⁶J. Kurkijärvi, D. Rainer, J. A. Sauls, *Can. J. Phys.* **65**, 1940

(1987).

⁷A. Millis, D. Rainer, and J. A. Sauls, *Phys. Rev. B* **38**, 4504 (1988).

⁸J. W. Serene and D. Rainer, *Phys. Rep.* **101**, 221 (1983).

⁹Magnetic terms of the form $\mathbf{m} \sim \hat{\mathbf{p}} \times \hat{\boldsymbol{\mu}}$ are disallowed if the Hamiltonian describing the metal and interface is invariant under reflections in a plane containing the interface normal, and under rotations about the normal $\hat{\mathbf{n}}$. See Ref. 7 for more details regarding the constraints imposed on S by various symmetry operations.

¹⁰E. V. Thuneberg, J. Kurkijärvi, and D. Rainer, *Phys. Rev. B* **29**, 3913 (1984).

¹¹Care must be taken in setting up the Newton iteration in order to ensure that the updating procedure converges. See W. Zhang, J. Kurkijärvi, and E. V. Thuneberg, *Phys. Lett.* **109A**, 2381 (1985).

¹²B. Ashauer, G. Keiselmann, and D. Rainer, *J. Low Temp. Phys.* **63**, 349 (1986).

- ¹³R. P. Groff and R. D. Parks, *Phys. Lett.* **22**, 19 (1966).
- ¹⁴J. E. Tkaczyk and P. M. Tedrow, *J. Appl. Phys.* **61**, 3368 (1987).
- ¹⁵The gap parameter $\Delta(T, \rho)$ defined by Eqs. (29)–(31) is not the true energy gap in the quasiparticle DOS, except for $\rho=0$. The true energy gap is shifted by the effective surface field $\pm\alpha$ as shown in Sec. VII.
- ¹⁶G. Sarma, *J. Phys. Chem. Solids* **24**, 1029 (1963).
- ¹⁷K. Maki and T. Tsuneto, *Prog. Theor. Phys.* **31**, 945 (1964).
- ¹⁸For clean superconductors in which the mean free path is long compared to the coherence length there is an intermediate transition from normal metal to a spatially varying state of the order parameter and spin density. The transition to the uniform superconducting state is first order. We discuss only the possibility of a transition from the normal metallic phase to the uniform superconductor. For more detail see P. Fulde, *Adv. Phys.* **22**, 667 (1973). This article also reviews the theory of high-field tunneling in thin superconducting films.
- ¹⁹P. M. Tedrow, J. T. Kucera, D. Rainer, and T. P. Orlando, *Phys. Rev. Lett.* **52**, 1637 (1984).
- ²⁰We can safely neglect the diamagnetic coupling to the magnetic field for thin films with $d \ll \lambda$, where λ is the London screening length.
- ²¹Y. Shapira, S. Foner, R. L. Aggarwal, and T. B. Reed, *Phys. Rev. B* **8**, 2316 (1973).
- ²²We note that the value of $M_0 = 0.19$ T calculated for $J = S = \frac{7}{2}$ EuO spins in an NaCl structure of cube size $a = 5.15 \text{ \AA}$ agrees well with the magnetization measured by Shapira *et al.* at their lowest temperatures and highest applied fields.
- ²³T. Penney, M. W. Shafer, and J. B. Torrence, *Phys. Rev. B* **5**, 3669 (1972).